Available online at www.sciencedirect.com
ScienceDirect
Journal of Hazardous Materials 157 (2008) 455–463
Journal of Hazardous Materials
www.elsevier.com/locate/jhazmat

Determination of the apparent rate constants of the degradation of humic substances by ozonation and modeling of the removal of humic substances from the aqueous solutions with neural network

Ensar Oguz[a,*], Ahmet Tortum[b], Bülent Keskinler[c]

[a] *Atatürk University, Environmental Engineering Department, 25240 Erzurum, Turkey*
[b] *Atatürk University, Civil Engineering Department, 25240 Erzurum, Turkey*
[c] *Gebze Institute of Technology, Environmental Engineering Department, 41400 Çayırova, Kocaeli, Turkey*

Received 16 June 2007; received in revised form 4 January 2008; accepted 7 January 2008
Available online 15 January 2008

Abstract

In this study, the degradation rate constants of humic substances by ozonation under the different empirical conditions such as ozone-air flow rate, ozone generation potential, pH, temperature, powdered activated carbon (PAC) dosage and HCO_3^- ions concentration were determined. The ozonation of humic substances in the semi-batch reactor was found to fit pseudo-first-order reaction. The values of apparent rate constant of humic substances degradation increased with the increase of initial ozone-air flow rates, ozone generation potential, pH, temperatures and PAC dosage, but decreased with the increase of HCO_3^- concentration of the solution. Using Arrhenius equation, the activation energy (E_a) of the reaction was found as 1.96 kJ mol^{-1}. The reaction of ozonation of humic substances under the different temperatures was defined as diffusion control according to E_a. The model based on artificial neural network (ANN) could predict the concentrations of humic substances removal from aqueous solution during ozonation. A relationship between the predicted results of the designed ANN model and experimental data was also conducted. The ANN model yielded determination coefficient of ($R^2 = 0.995$), standard deviation ratio (0.065), mean absolute error (4.057) and root mean square error (5.4967).

Keywords: Ozonation; Apparent rate constants; Neural network; Humic substances

1. Introduction

Humic substances (HSs) are the predominant type of natural organic matter present in ground and surface waters. Humic substances are generally classified as humic acids (HAs), fulvic acids (FAs) and humin. HA are comprised of high-molecular-weight organic substances that are soluble in alkaline media and insoluble in acidic media, whereas FA comprise moderate-molecular-weight organic substances which are soluble at all pH values. Humic substances impart undesirable color and act as precursors for undesirable trihalomethane formation during the chlorination process, their presence in drinking water supplies causes problems [1,2]. Humic substances create a world wide problem in drinking water supply as they constitute a yellow color in drinking water. Humic substance is the name for a cocktail of organic molecules that originate from biological degradation of dead plants and animals in the soil and surface water. Humic substances contain a variety of functional groups like unsaturated bonds and aromatic groups. Further ketonic, alcoholic and carboxylic groups and aldehydes are found in HS molecules. A characteristic feature of humic substances is their low biodegradability. Being a product of microbial degradation processes, it has lost its value as energy source for microorganisms [3].

In the US Environmental Protection Agency (USEPA), in potable water supplies, the maximum contaminant level for trihalomethanes (THMs) and five haloacetic acids (HAA5) is defined as 60 and 80 μg/l, respectively [4].

* Corresponding author. Tel.: +90 442 231 4601.
E-mail address: eoguz@atauni.edu.tr (E. Oguz).

0304-3894/$ – see front matter © 2008 Elsevier B.V. All rights reserved.
doi:10.1016/j.jhazmat.2008.01.018

In addition to the conventional treatments such as coagulation, precipitation, filtration, ion-exchange, use of activated carbon, or biological treatment [5,6], advanced photocatalytic methods have been applied for reducing the organic content of water [7–9].

Ozone has been demonstrated to oxidize a variety of inorganic matters, HS and toxicity contaminants found in drinking water [10]. Thus, the ozonation method is preferred in many instances for treating drinking water to achieve both disinfection and oxidation [10]. The ozone oxidation is accomplished in two pathways: direct oxidation by molecular ozone and indirect oxidation by hydroxyl radical [11]. The direct ozone oxidation reactions are highly selective but relatively slow attacking the unsaturated electron-rich bonds contained in specific functional groups, aromatics, olefins and amines [12]. In comparison, the indirect reaction has a relatively low selectivity but a quick reaction rate by hydroxyl radicals, which are generated by decomposition of ozone molecule [13,14]. The hydroxyl radicals can oxidize regular organic substrates, microorganisms and NH_3-nitrogen.

The objective of this investigation is to study the degradation kinetics of the HS and to define the apparent rate constants by ozonation under the different empirical conditions such as ozone-air flow rates from 5 to 15 l/min (in which the ozone gas flow rate produced by system is 144, 289 and 432 mg/min), ozone generation potential (96–170 V), pH (4–12), temperatures (14–60 °C), powdered activated carbon (PAC) (0–1 g in solution of 250 mL) and HCO_3^- (0–2000 mg/l). In addition to the apparent rate constants, the modeling of artificial neural network (ANN) was used to predict the concentrations of HS removal from aqueous solution during ozonation. A relationship between the predicted results of the designed ANN model and experimental data was also conducted. At the result of this study, the determination coefficient (R^2), standard deviation ratio, mean absolute error and root mean square error in the modeling of ANN were defined as 0.995, 0.065, 4.057 and 5.4967, respectively.

2. Materials and methods

2.1. Preparation of the solutions of HS

As a model pollutant, HS bought from Sigma–Aldrich Co. have been used in this study and its properties were given in Table 1 [15].

The most probable structures in humic substances are residues of phenolic structures in their core, and functional groups such as phenolic hydroxylgroups, carboxylgroups and aminogroups in the peripheral part of the humic macromolecules [16,17]. Structures of hypothetical molecules of humic substance for potential use in their immobilization have been shown in Fig. 1 [16]. Recent studies have shown that carboxylic and phenolic groups in humic substances are most active and they complex and reduce metal ions at different pH values [18].

HS of 300 mg was dissolved in 1 l of distilled water and used as stock solution of which the value of initial pH was 10. The concentration of HS in the stock solution was measured, and the solution was used for further experimental solution preparation. The initial humic substances' concentrations used in kinetic studies were 100, 200 and 300 mg/l, respectively.

Table 1
Properties of the HS

Element	(%)
C	39.3
H	4.43
N	0.68
Na	0.767
S	0.25
Fe	0.13
Ca	0.12
Mg	0.1091
P	0.0215
Li	0.0003

Double-beam spectrophotometer (Shimadzu UV-160 A) was used to measure the value of absorbance of humic substance. It was defined that humic substances as a function of color gave a peak at 315 nm. Humic substance removal capacity was determined by absorbance measurements at the maximum visible absorbance wavelength of 315 nm. All the samples to measure humic substances' concentrations was analysed at 315 nm.

Distilled water was used to prepare and dilute the synthetic solutions containing humic substance. The initial pH was adjusted to a desired value using NaOH or H_2SO_4.

2.2. Preparation of HCO_3^- solutions

HCO_3^- solutions of 0, 1000 and 2000 mg/l used in this study were prepared from $NaHCO_3$ (Merck).

2.3. Powdered activated carbon

A commercial activated carbon from Merck was used throughout this study. The surface area of the PAC particles was measured by BET method at 77 K using a Quantachrome QS-17 model apparatus. The surface area of the PAC was 455 m^2/g [19].

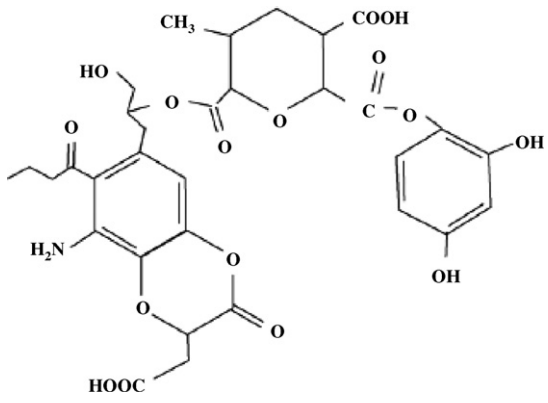

Fig. 1. Functional structures of humic substances [16].

2.4. Ozonation studies

The experimental set-up includes an air dryer, compressor, ozone generator and semi-batch reactor having 1 l of volume. The air dryer consisted of a column filled with a high adsorptive anhydrous $CaCl_2$. Ozone was generated using an ozonizer Model OG-24. The ozone–oxygen mixture was then fed into the contact place through a porous plate gas sparger placed into the semi-batch reactor's base [20–22].

The ozonation reactor has been built by a glass column of 7-cm diameter, 40-cm height with a water-cooling jacket keeping the reactor at constant temperature. A HS solution of 250 ml was used for each batch ozonation. A magnetic stirrer was used with the gas diffuser for sufficient circulation of the HS solution.

Ozone was generated from air, and was supplied into the system through an Opal OG-24 model ozonizer at the rates of 5, 10 and 15 l/min. The application rates of ozonation for the reactor are 144, 289 and 432 mg/min, respectively. Ozonation was performed in a cylindrical semi-batch glass reactor of which volume is 1 l. HS were ozonated for 18 min in the semi-batch reactor.

3. Results

3.1. The determination of apparent rate constants by ozonation

The ozonation of HS was considered as a second-order reaction with first-order relative to the humic substances [HS] and ozone [O_3] concentrations. The rate of HS disappearance could be formulated by the folowing equation:

$$V = -\frac{\mathrm{dHS}}{\mathrm{d}t} = k[\mathrm{O_3}][\mathrm{HS}] \quad (1)$$

where k is the second-order rate constant. When the amount of ozone is in excess, the reaction is pseudo-first-order with respect to the HS [23]. In this study, the pseudo-first-order trend was observed in each of the experimental runs. Thus, ozone concentration could be considered constant during reaction and the expression of the rate of HS degradation was given by the following equation:

$$V = -\frac{\mathrm{dHS}}{\mathrm{d}t} = k\prime[\mathrm{HS}] \quad (2)$$

where k' is apparent first-order kinetic constant (min^{-1}). Therefore, a plot of $\ln[\mathrm{HS_o}/\mathrm{HS}]$ versus the reaction time led to a straight line from which k' could be determined.

The removal of HS process kinetics from the synthetic aqueous solutions was investigated under the different experimental conditions. The values of apparent rate constants were shown in Figs. 1–6. At different empirical conditions, the empirical results of ozonation of HS have showed that the ozonation reaction kinetics followed a pseudo first-order reaction ($R^2 \approx 1$).

As seen in Fig. 2, the apparent rate constants in the HS removal increased with the increase of ozone-air flow rate from 5 to 15 l/min and the value of apparent rate constant was maximum at the value of 15 l min^{-1}.

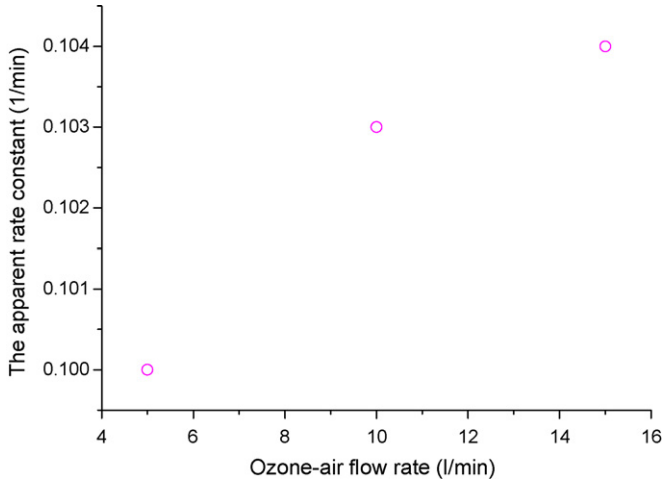

Fig. 2. The change of apparent rate constants *vs*. ozone-air flow rate (HS_o: 300 mg/l, *T*: 18 °C, O_3: 1.4%, pH: 10, HCO_3^-: 0 mM, H_2O_2: 0 mM and PAC: 0 g).

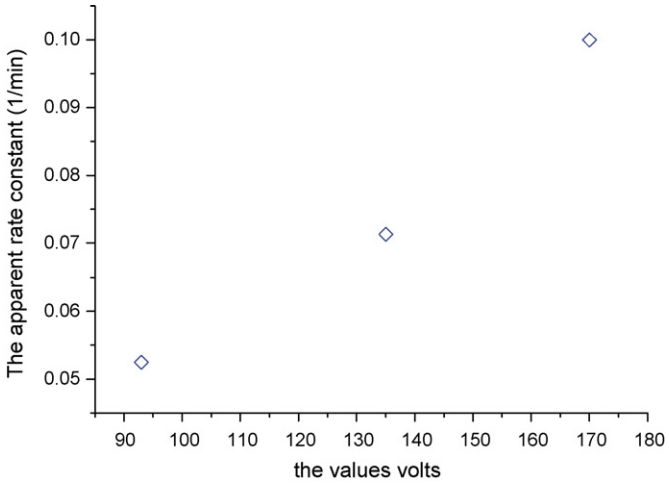

Fig. 3. The change of apparent rate constants *vs*. ozone generation potential (HS_o: 300 mg/l, ozone application rate: 144 mg/min, *T*: 18 °C, *Q*: 5 l min^{-1}, pH: 10, HCO_3^-: 0 mM, H_2O_2: 0 mM and PAC: 0 g).

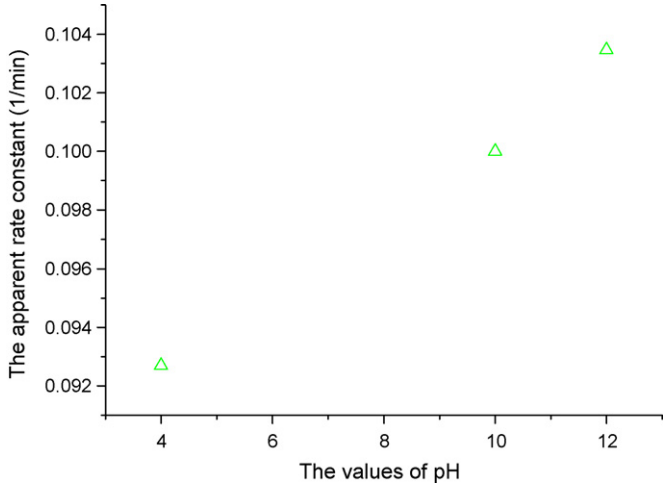

Fig. 4. The change of apparent rate constants *vs*. the values of pH (HS_o: 300 mg/l, ozone application rate: 144 mg/min, *T*: 18 °C, *Q*: 5 l min^{-1}, O_3: 1.4%, HCO_3^-: 0 mM, H_2O_2: 0 mM and PAC: 0 g).

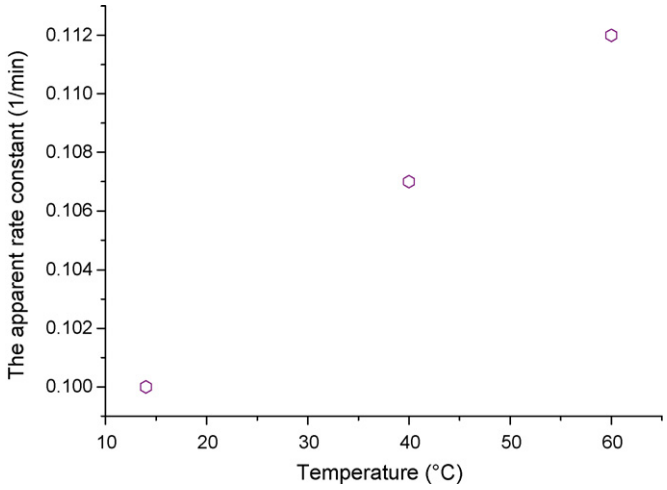

Fig. 5. The change of values of apparent rate constants *vs*. the temperature of solution (HS_o: 300 mg/l, ozone application rate: 144 mg/min, pH: 10, *Q*: 5 l min^{-1}, O_3: 1.4%, HCO_3^-: 0 mM, H_2O_2: 0 mM and PAC: 0 g).

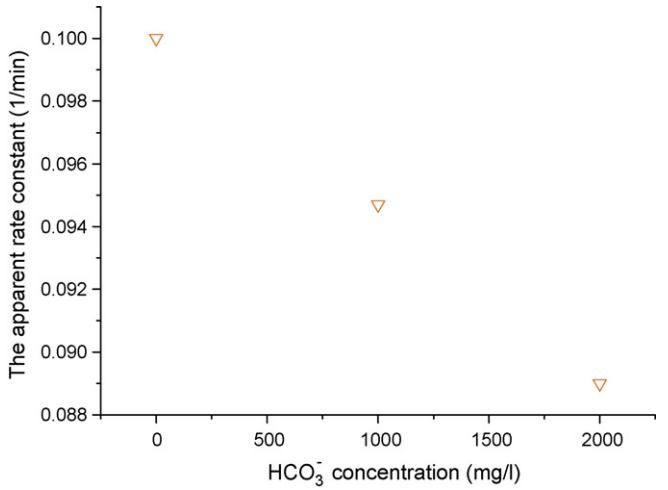

Fig. 7. The change of apparent rate constants *vs*. the HCO_3^- ion concentration (HS_o: 300 mg/l, ozone application rate: 144 mg/min, pH: 10, *Q*: 5 l min^{-1}, O_3: 1.4%, H_2O_2: 0 mM and PAC: 0 g).

Fig. 3 shows that the change in the apparent rate constants with the increase of ozone generation percentages (from 96 to 170 V). The apparent rate constants increased with the increase of ozone generation potential. The more molecules of O_3 occurred with the increase of ozone generation potential. O_3 molecules attacked to the double bonds in the HS then these bonds were broken by ozone. With the more HS degradation, the more HS were removed from aqueous solution and as seen from Fig. 3, the value of apparent rate constant was defined as maximum at the value of 170 V.

At various initial pH values (4, 10 and 12), the change of apparent rate constants of HS degradation by ozonation were investigated and shown in Fig. 4. The apparent rate constants of HS were found to increase with the increase of pH during ozonation time. As known, ozone oxidation pathways include direct oxidation by ozone or radical oxidation by $OH^\bullet$ radical. Direct oxidation by ozone is more selective and predominates under acidic conditions, while radical oxidation with $OH^\bullet$ radical is less selective and predominates under basic conditions. Since the oxidation potential of hydroxyl radicals is 2.08 V and much higher than that of the ozone molecule (1.86 V), direct oxidation is slower than radical oxidation. The increase of solution pH showed a positive enhancement of the ozone oxidation of HS during ozonation. At various initial pH values (4, 10 and 12), the ozonation of the HS was examined, and the values of apparent rate constant increased with the increase of pH as seen from Fig. 4.

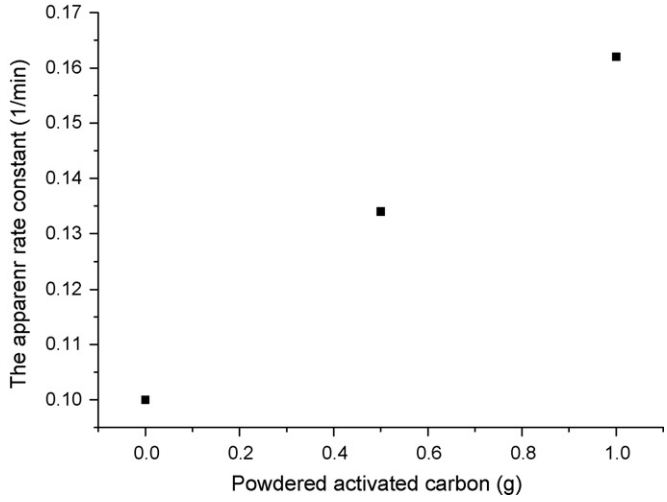

Fig. 6. The change of apparent rate constants *vs*. the PAC dosages used in the solution (HS_o: 300 mg/l, ozone application rate: 144 mg/min, pH: 10, *Q*: 5 l min^{-1}, O_3: 1.4%, HCO_3^-: 0 mM and H_2O_2: 0 mM).

As seen Fig. 5, the values of apparent rate constant of HS degradation by ozonation increased with the increase of temperature from 14 to 60 °C. After an ozonation of 18 min, the biggest value of apparent rate constant connected with temperature of the solution was found at the value of 60 °C. It was thought that this increase in the apparent rate constants arises from the increase of the reaction rate which increased with the increase of temperature of solution.

At the different PAC dosages such as 0, 0.5 and 1 g in the solution of 250 ml, the values of apparent rate constant of HS degradation by ozonation were shown in Fig. 6. These values increased with the increase of PAC dosage from 0 to 1 g. In the present study, it was thought that PAC played an important role as adsorbent [22]. The PAC used to remove HS from aqueous solution has quite a positive effect on the treatment of HS.

Fig. 7 shows the values of apparent rate constant in the O_3/HCO_3^- process. HCO_3^- ions in the O_3/HCO_3^- process scavenge occurring $OH^\bullet$ radicals during ozonation. Bicarbonate ions are the principal consumer of the hydroxyl radicals, particularly when relatively high concentrations of bicarbonate are present in water, HCO_3^- ions react with hydroxyl radicals to generate bicarbonate radicals ($HCO_3^{\bullet -}$). It was reported that bicarbonate ions scavenge hydroxyl radicals to produce intermediates not releasing a radical-type chain carrier, thereby quenching the radical-type chain reaction [24]. Because of the scavenging effect of bicarbonate ions on the $OH^\bullet$ radicals, the values of apparent rate constant of HS by ozonation decreased

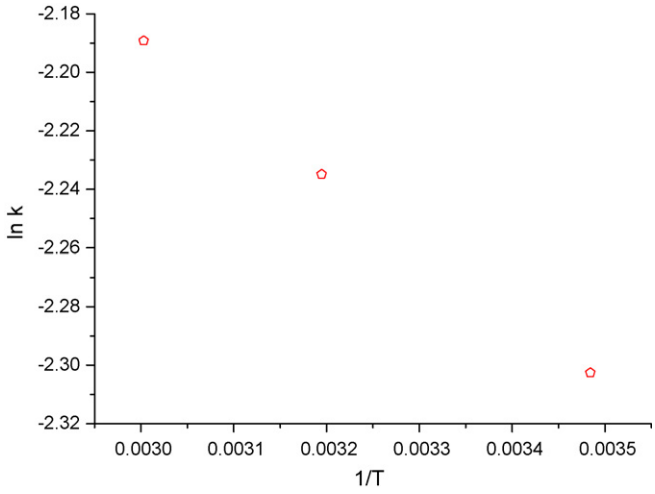

Fig. 8. The plot of ln (*k*) *vs*. (1/*T*).

with the increase of HCO_3^- ion concentration. When HCO_3^- ions were not used in the aqueous solution, the value of apparent rate constant received a maximum value as seen from Fig. 7.

Fig. 8 shows the plot of ln (*k*) versus (1/*T*). Arrhenius equation used to define the value of activation energy (E_a) is given by the following equation:

$$\ln k = \ln A - \frac{E_a}{R}\frac{1}{T} \quad (3)$$

where *k*, *A*, E_a, *R* and *T*, are reaction rate constant, pre-exponential factor, activation energy ($J\,mol^{-1}$), ideal gas constant ($8.314\,J\,mol^{-1}\,K^{-1}$) and temperature (K), respectively. A plot of ln *k* versus 1/*T* would result in a straight line with a slope of ($-E_a/R$) and intercept of ln *A* as seen from Fig. 8.

The value of E_a calculated using Arrhenius equation was found as $1.96\,kJ\,mol^-$ which was smaller than the value of $20\,kJ\,mol^{-1}$. Thus, the reaction of ozonation of HS under the different temperatures such as 287, 313 and 333 K was defined as diffusion control.

3.2. Application of artificial neural network

The linear model presents the disadvantage to give a relationship very satisfying for an oxidation study, subject to the real independence of variables. In fact, it is reasonable to consider that such variables are not totally independent. ANN approach seems to be completely suitable to the problems where the relations between variables are not linear and complex [25].

ANNs are direct inspiration from the biology of human brain, where billions of neurons are interconnected to process a variety of complex information, accordingly, a computational neural network consists of simple processing units called neurons. Each neuron (a processing element) is linked to its neighbors with varying strengths. The strength of connection between two neurons is called *weight* and is represented by coefficients of connectivity *w*. The basic of an artificial neuron used in this study is shown in Fig. 9. As shown in Fig. 9, a neural net is a parallel interconnected structure consisting of: (1) input layer of neuron (independent variables), (2) a number of hidden layers and (3) output layer (dependent variables). The number of input and output neurons is determined by the nature of the problem. The hidden layers act like feature detectors and in theory, there can be more than one hidden layer. Universal approximation theory suggests that a network with a single hidden layer with a sufficiently large number of neurons can interpret any input–output structure [26]. Input neurons accept the input data characterizing a given observation (experiment). Output neurons yield the predicted (expected) value. A neuron sums the product of each connection weight (w_{jk}) from a neuron (*j*) to the neuron (*k*) and input (x_j) and the additional weight called as the bias to get the value of sum for the neuron (*k*):

$$\text{sum}\,k = \sum w_{jk}x_j + \text{bias}_k \quad (4)$$

The sum of the weighted inputs is further transformed with a *transfer function* to get the output value, there are several

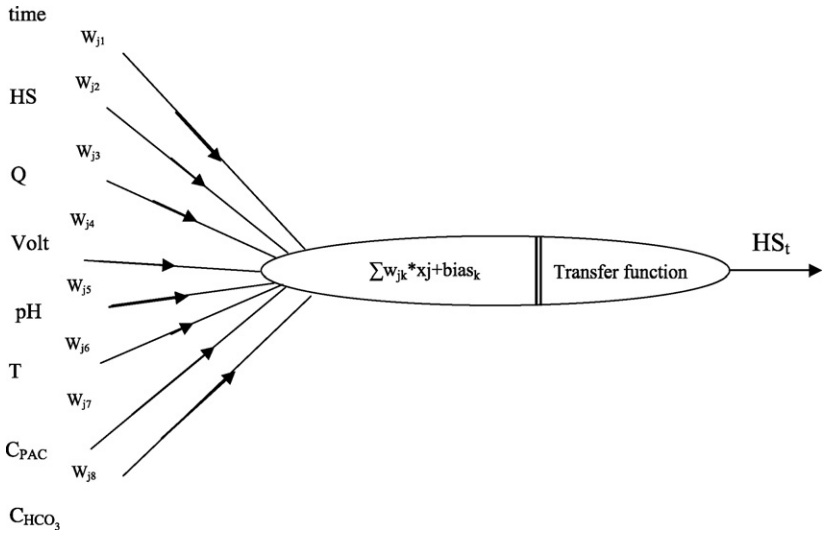

Fig. 9. Basic structure of an artificial neuron—the unit of the artificial neural network.

transfer functions; the most common is the sigmoidal function [27].

To find suitable ws and biases for each neuron, a process training is essential; it is the first step of building an ANN, training means that the weights are corrected to produce prespecified ("correct", known from experiments) target values, the training requires sets of pairs (X_S, Y_S) for input: the actual input into the network is a vector (X_S), and the corresponding target is labelled (Y_S) after successful training. When correct values of Y_S for each vector of X_S from the training set are obtained, it is hoped that the network will give correct predictions of Y for any new object of X, according to the ANN model fundamentals, with use of more data for training the network, better result would be obtained. The most utilized training method for multilayered neural network is called *back propagation*, in this study; one hidden layer was used. Information about errors (differences between target and predicted values) is filtered back through the system and is used to adjust the connections between the layers, thus performance improves. In the early standard algorithm, random initial set of weights were assigned to the neural network, and then by considering the input data, weights were adjusted so the output error would be on its minimum [28].

In this study, one-layered back propagation neural network was used for modeling of the removal of HS with ozonation (Fig. 9). In the present work, the input variables to the neural network are as follows: the treatment time (t), the concentration of initial HS, PAC, ozone-air flow rate, ozone generation potential, pH, temperature and HCO_3^- ions concentration. The concentration of removal of HS as a function of reaction time was chosen as the experimental response or output variable.

In order to model the HS concentrations with ANN, Statistica software program was used. The coefficient of determination (R^2), the root mean square error (RMSE), the standard deviation ratio (SDR), and the mean absolute error (MAE) are the main criterions that are used to evaluate the performance of ANN, they are defined as follows:

$$R = \frac{\left[n\left(\sum \text{obs} - \text{pre}\right) - \left(\sum \text{obs}\right)\left(\sum \text{pre}\right)\right]}{\sqrt{\left[n\sum \text{obs}^2 - \left(\sum \text{obs}\right)^2\right] \times \left[n\sum \text{pre}^2 - \left(\sum \text{pre}\right)^2\right]}} \quad (5)$$

$$\text{RMSE} = \sqrt{\frac{(\text{obs} - \text{pre})^2}{n}} \quad (6)$$

$$\text{SDR} = \frac{\sqrt{n\sum \text{obs}^2 - \left(\sum \text{obs}\right)^2/n(n-1)}}{\sqrt{n\sum \text{error}^2 - \left(\sum \text{error}\right)^2/n(n-1)}} \quad (7)$$

$$\text{MAE} = \frac{\sum |\text{obs} - \text{pre}|}{n} \quad (8)$$

Low values of RMSE, SDR and MAE satisfy the statistical evaluation of prediction for the validation [29,30].

Table 2
Shift and scale factors

Parameters	Shift	Scale
t	0	0.05556
HS_o	−0.5	0.005
pH	−0.5	0.125
Q	0	0.06667
Volt	0	0.005882
T	−0.3043	0.02174
HCO_3^-	0	0.0005
PAC	0	1
HS_t	−0.0453	0.003484

Before the network was trained, the input and the output data had been normalized; the scale and shift factors which were used in every input and output were given in Table 2.

The weight coefficients and the biases given in Table 3 are the values obtained for the normalized data, in order to determine the actual (experimental) HS concentration, an inverse transformation on this data must be performed by using shift and scale factors.

After long training phases, the best result was obtained from the Levenberg–Marquardt algorithm. The hyperbolic tangent function in the hidden layer and the linear activation function in the output layer were used in the model. It was observed that the optimal network was found to be eight inputs, one hidden layer with ten neurons and one output layer, the optimal network architecture ($8 \times 10 \times 1$) is shown in Fig. 9.

Sensitivity analysis is a technique to assess the relative contribution of the input variables to the performance of a neural network by testing the neural network when each input variable is unavailable, this indicates that input variables are considered most important by particular neural network, if the ratio is one or lower, making the variable unavailable either has no effect on the performance of the network, or actually enhances it, because ratios of input parameters of the model are more than one, all input variables are meaningful. The results of the sensitivity analysis were given in Table 4.

Table 3
Connection weights and biases

Bias	2.1	2.2	2.3	2.4	2.5
			b_1		**b_2**
	−3.22354	−7.73605	7.630017	−2.68242	−1.70313
			w_1		
1.1	4.319147	6.302514	2.132686	1.585571	
1.2	−3.75474	−9.05241	−1.7553	1.667741	
1.3	−0.00325	0.038797	0.553008	1.973945	
1.4	1.799366	5.531177	0.140772	−5.31505	
1.5	−0.5213	−3.08825	7.542647	−20.0641	
1.6	0.297161	0.72685	0.576841	−1.03173	
1.7	−0.01387	−0.1432	−0.6086	−3.4185	
1.8	0.571225	1.897449	3.273081	3.954508	**w_2**
2.1					−1.92635
2.2					0.606859
2.3					−0.3781
2.4					−0.121

Table 4
Sensitivity analysis results

	t	HS_o	pH	Q	Volt	T	HCO_3^-	PAC
Rank	1	3	8	5	2	6	7	4
Ratio	12.43	4.87	1.05	1.42	6.46	1.24	1.10	2.38

Table 5
The statistical values of ANN model (8 × 4 × 1)

R^2	0.995
SDR	0.065
RMSE	5.496
MAE	4.057

When Table 4 is examined, it is easy to see that the most important parameter that affects the removal of concentration of HS is the treatment time (t), volt, initial HS concentration, PAC, ozone-air flow rate, temperature (T), HCO_3^- and pH, respectively. At the result of this study, the general equation obtained from the optimal network was given as following:

$$HS_t = f_2\left(\mathbf{w}_2 f_1\left(\mathbf{w}_1\begin{bmatrix} t \\ HS_o \\ pH \\ Q \\ Volt \\ T \\ HCO_3^- \\ PAC \end{bmatrix} + \mathbf{b}_1\right) + \mathbf{b}_2\right) \quad (9)$$

where $\mathbf{w}_1$ and $\mathbf{w}_2$ are the weight matrices, $\mathbf{b}_1$ and $\mathbf{b}_2$ are the biases vectors and their values can be taken from Table 3.

Under the different experimental conditions along the reaction time, the interpretation of the experimental results was based on the fitting of neural network models for predicting the removal of concentration of HS by ozonation, the proposed model based on artificial neural network (ANN) could predict the HS_t concentration during ozonation time, a comparison between the predicted results of the designed ANN model and experimental data was also conducted.

According to the ANN model fundamentals, with use of more data for training the network, better result would be obtained. In the early standard algorithm, random initial set of weights were assigned to the neural network, and then by considering the input data, weights were adjusted so the output error would be on its minimum. The results from general ANN modeling were shown in Fig. 10.

The general model from the ANN belonging to all of the parameters (treatment time, HS concentration, ozone-air flow rates, ozone generation potential, pH, temperature, PAC, HCO_3^-) was given in Fig. 10.

The results of statistical analysis of ANN are summarized in Table 5. It was seen that the ANN model has determination coefficient of (0.995), SDR of (0.065), RMSE of (5.496) and MAE of (4.057). The results obtained in this model indicate that ANN model has the ability to predict the removal of HS concentration.

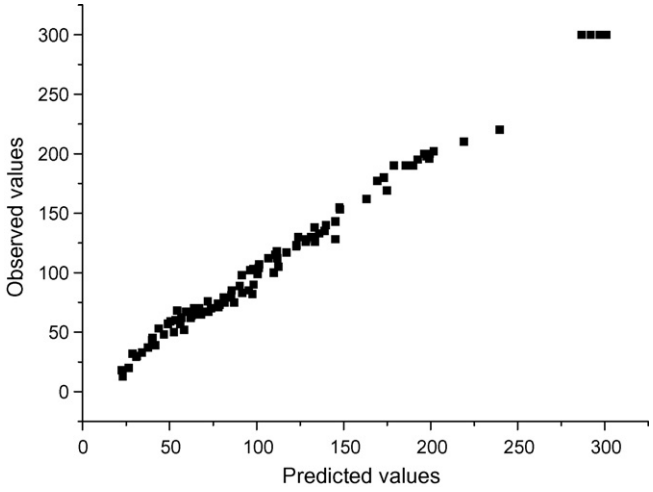

Fig. 10. Comparison between observed and predicted values relating to general modeling ($R^2 = 0.995$).

In the ANN modeling, it was seen that the error distributions of the model do not show complete normal distribution. Almost every value predicted in the model and the distribution of the errors is very close to the zero line as seen from Fig. 11. Error distributions do not show complete normal distribution. It was also observed that almost every value predicted in the model and the distribution of the errors is not in the line of zero.

The error histogram is not widely open to the right and left directions, the zero error frequency is high as seen from Fig. 12. The zero error frequency is high and also in the model the predicted values together with the observed values are in good agreement. Moreover, the explanatory variables in the models to explain the dependent variable are found to be satisfactorily sufficient.

In a good model, the residuals show normal distribution. The assumption of normality can be checked by plotting the residual versus expected normal values. The normal probability plot of the residuals for ANN is shown in Fig. 13. Fig. 13 shows an approximately linear behavior, indicating that the residuals follow an approximately normal distribution.

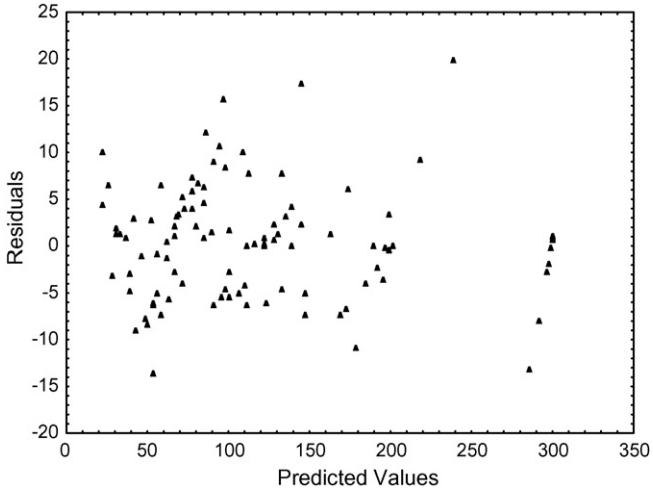

Fig. 11. Residuals *vs*. predicted values.

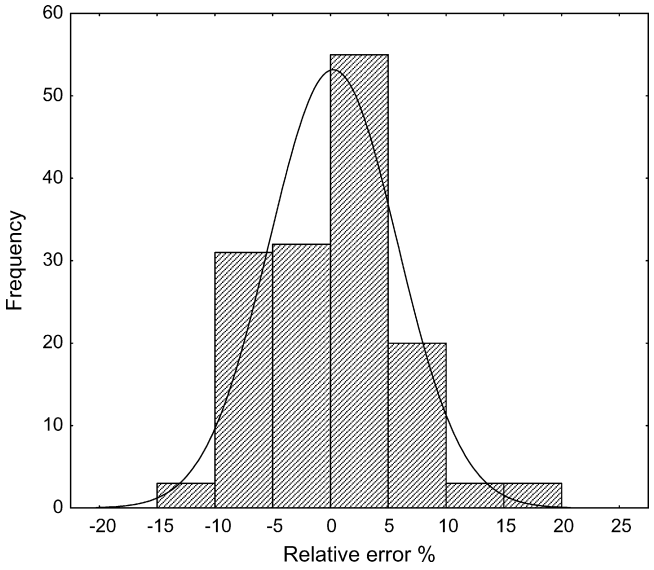

Fig. 12. Relative error distribution.

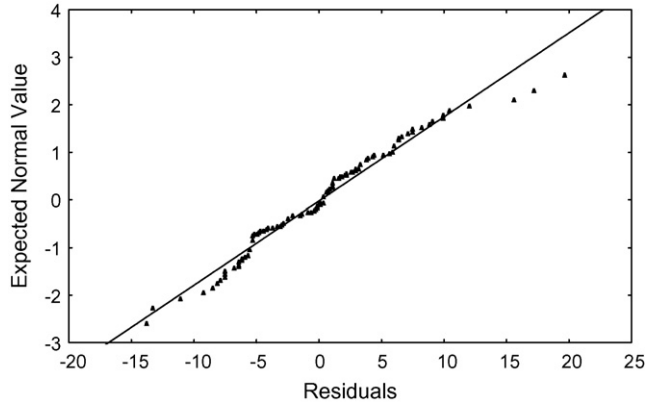

Fig. 13. Normal probability plot of residuals.

4. Conclusion

At the result of this study, it was defined that the ozonation of HS fitted the pseudo-first-order reaction. The values of apparent rate constant of HS degraded by ozonation increased with the increase of ozone-air flow rate, temperature, pH, ozone generation potential and PAC but decreased with the increase of HCO_3^- ions concentration of the solution. At a high pH, the ozonation of HS contributed to increase of the apparent rate constant because of occurring free hydroxyl radicals. Using Arrhenius equation, the activation energy (E_a) of the reaction was found as 1.96 kJ mol^{-1}. The reaction of ozonation of HS under the different temperatures (287, 313 and 333 K) was defined as diffusion control because the value of E_a is smaller than 20 kJ mol^{-1}. Artificial neural network modeling has been used to investigate the cause–effect relationship in the ozonation studies of HS. The ANN model could describe the behavior of the ozonation reaction system (O_3/PAC, O_3/HCO_3^- processes) with the adopted experimental conditions. Simulation based on the ANN model can then be performed in order to estimate the behavior of the system under the different conditions. The model based on ANN could predict the concentrations of HS removal from aqueous solution during ozonation. A relationship between the predicted results of the designed ANN model and experimental data was also conducted. At the result of ANN model, the values of determination coefficient (R^2), standard deviation ratio, mean absolute error and root mean square error were obtained as 0.995, 0.065, 4.057and 5.496, respectively.

References

[1] J.J. Rook, Formation of haloforms during chlorination of natural waters, Water Treat. Exam. 23 (2) (1974) 234–243.
[2] P.C. Singer, Humic substances as precursors for potentially harmful disinfection by-products, Water Sci. Technol. 40 (9) (1999) 25–30.
[3] H. Ødegaard, Removal of humic substances from water, Water Sci. Technol. 40 (1999) 9.
[4] Federal Register, Revisions to the Interim Enhanced Surface Water Treatment Rule (IESWTR), The Stage 1 Disinfectants and Disinfection Byproducts Rule (Stage 1DBPR), and Revisions to State Primacy Requirements to Implement the Safe Drinking Water Act (SDWA) Amendments, January 16, 66 (10), 2001.
[5] M. Alborzfar, G. Jonsson, C. Gron, Removal of natural organic matter from two types of humic ground waters by nanofiltration, Water Res. 32 (10) (1998) 2983–2994.
[6] R. Kati, P. Vaisanen, M.S. Metasa, M. Kutovaara, M. Nystrom, Characterization and removal of humic substances in ultra and nanofiltration, Desalination 118 (1) (1998) 273–283.
[7] O. Legrini, E. Oliveros, A.M. Braun, Photochemical processes for water treatment, Chem. Rev. 93 (2) (1993) 671–698.
[8] B.R. Eggins, F.L. Palmer, J.A. Byrne, Photocatalytic treatment of humic substances in drinking water, Water Res. 31 (5) (1993) 1223–1226.
[9] W. Hongbin, X. Dimir, Photo-oxidation of humic acid in aqueous solution catalysed by a TiO_2 film, Sci. Circum. 18 (2) (1998) 161–166.
[10] R.G. Rice, C.M. Robson, G.W. Miller, A.G.M. Hill, Use of ozone–bromide reactions, J. Am. Water Works Assoc. 85 (1981) 63–72.
[11] J. Hoigne, H. Bader, The role of hydroxyl radical reactions in ozonation processes in aqueous solutions, Water Res. 10 (1976) 377–386.
[12] J. Hoigne, H. Bader, Rate constants of reactions of ozone with organic and inorganic compounds in water. II. Dissociation organic compounds, Water Res. 17 (1983) 185–194.
[13] J. Hoigne, Inter-calibration of OH radical sources and water quality parameters, Water Sci. Technol. 35 (1997) 1–8.
[14] J. Prado, J. Arantegui, E. Chamarro, S. Esplugas, Degradation of 2,4-D by ozone and light, Ozone-Sci. Eng. 16 (1994) 235–245.
[15] Y.Ş. Yıldız, A.S. Koparal, Ş. Irdemez, B. Keskinler, Electrocoagulation of synthetically prepared waters containing high concentration of NOM using iron cast electrodes, J. Hazard. Mater. 139 (2) (2006) 373–380.
[16] M. Klavins, L. Eglite, Immobilization of humic substances, Colloids Surf. A: Physicochem. Eng. 203 (2002) 47–57.
[17] J. Duan, J. Wang, N. Graham, F. Wilson, Coagulation of humic acid by aluminum sulphate in saline water conditions, Desalination 150 (2002) 1–14.
[18] X. Lu, Z. Chen, X. Yang, Spectroscopic study of aluminum speciation in removing humic substances by Al coagulation, Water Res. 33 (15) (1999) 3271–3280.
[19] E. Oguz, B. Keskinler, Determination of adsorption capacity and thermodynamic parameters of the PAC used for bomaplex red CR-L dye removal, Colloids Surf. A: Physicochem. Eng. Aspects 268 (2005) 124–130.
[20] E. Oguz, B. Keskinler, Z. Celik, Ozonation of aqueous Bomaplex Red CR-L dye in a semi-batch reactor, Dyes Pigments 64 (2005) 101–108.
[21] E. Oguz, B. Keskinler, C. Celik, Z. Celik, Determination of the optimum conditions in the removal of Bomaplex Red CR-L dye from the textile wastewater using O_3, H_2O_2, HCO_3^- and PAC, J. Hazard. Mater. B 131 (2006) 66–72.
[22] E. Oguz, B. Keskinler, Comparison among O_3, PAC adsorption, O_3/HCO_3^-, O_3/H_2O_2 and O_3/PAC processes for the removal of Bomaplex

Red CR-L dye from aqueous solution, Dyes Pigments 74 (2007) 329–334.
[23] C.C. David Yao, W.R. Haag, Rate constants for direct reactions of ozone with several drinking water contaminants, Water Res. 25 (1991) 761–773.
[24] J. Hoigne, Chemistry of Aqueous Ozone and Transformation of Pollutants by Ozonation and Advanced Oxidation Processes. The Handbook of Environmental Chemistry 5 (Part C), Springer, Berlin, Heidelberg, Germany, 1998.
[25] L. Bernard, P. Bernard, G. Karine, B. Florence, J.P. Croue, Modeling of bromate formation by ozonation of surface waters in drinking water treatment, Water Res. 38 (2004) 2185–2195.
[26] V.K. Pareek, M.P. Brungs, A.A. Adesina, R. Sharma, Artificial neural network modeling of a multiphase photodegradation system, J. Photochem. Photobiol. A 149 (2002) 139–146.
[27] J. Zupan, J. Gasteiger, Neural Networks in Chemistry and Drug Design, Wiley–VCH, Weinheim, 1999.
[28] J. Pazourek, D. Gajdŏsová, M. Spanilá, M. Farková, K. Novotná, J. Havel, Analysis of polyphenols in wines: correlation between total polyphenolic content and antioxidant potential from photometric measurements prediction of cultivars and vintage from capillary zone electrophoresis fingerprints using artificial neural network, J. Chromatogr. A 1081 (2005) 48–54.
[29] S. Çelik, Ö. Tan, Determination of preconsolidation pressure with artificial neural network, Civil Eng. Environ. Syst. 22 (4) (2005) 217–231.
[30] A. Tortum, The modeling of mode choices of intercity freight transportation with the artificial neural networks and integrated neuro-fuzzy system, Ph.D. Thesis, Atatürk University, 2003, in Turkish.